Joint Capacity, Flow and Rate Allocation for Multiuser Video Streaming over Wireless Ad-Hoc Networks

Sachin Adlakha
Wireless Systems Laboratory
Department of Electrical Engineering
350 Serra Mall
Stanford, CA 94305 U.S.A
Email: adlakha@stanford.edu

Xiaoqing Zhu, Bernd Girod
Information Systems Laboratory
Department of Electrical Engineering
350 Serra Mall
Stanford, CA 94305 U.S.A
Email: {zhuxq, bgirod} @stanford.edu

Andrea J. Goldsmith
Wireless Systems Laboratory
Department of Electrical Engineering
350 Serra Mall
Stanford, CA 94305 U.S.A
Email: andrea@stanford.edu

***Abstract*— Simultaneous support of multiple delay-critical application sessions such as multiuser video streaming require a paradigm shift in the design of ad-hoc wireless networks. Instead of the conventional layered approach, *cross-layer* optimization is needed for more efficient resource allocation, across the protocol stack and among multiple users. In this work, we extend our previous effort in joint capacity and flow assignment at the MAC and network layers, to include rate allocation at the application layer of each user. The proposed optimization aims to minimize the tradeoff between encoded video quality of all users versus overall network congestion. Compared to a scheme with oblivious layers, where capacity, flow and video rates are assigned individually, simulation results show significant performance gain of our proposed cross-layer approach, in terms of maximum sustainable rate and quality of the video streams.**

I. Introduction

A wireless ad-hoc network is a collection of wireless nodes that self-configure to form a network. Each node is either a transmitter, a receiver or a relay. Such a system is compelling for scenarios where communication infrastructure is either too costly or not feasible to be deployed. In industrial automation, for instance, the capability of wireless networking among sensors and actuators is an attractive means of cost reduction. Another example is search-and-rescue missions, where the availability of audiovisual communications can potentially save more lives in an infrastructure-less environment. These applications are by no means exhaustive but point to some potential areas for which the design of ad-hoc wireless networks are of great interest.

The flexibility promised by wireless ad-hoc networks also presents new design challenges. Each node needs to communicate in a multi-hop manner to its intended destination. The wireless medium inherently suffers from interference from other transmitters, multipath fading and shadowing. The lack of infrastructure requires that networking tasks, such as neighbor discovery and routing, be performed in a distributed manner. This decentralized control along with the hostile nature of underlying wireless links makes it extremely difficult to support delay-critical applications such as real-time media streaming. Varying channel conditions, node mobility, link failures, etc may cause significant quality degradation in delay-sensitive applications such as voice and video. These unique challenges have led to a paradigm shift in the design of wireless ad-hoc networks. In contrast to traditional layered paradigm where each layer is designed independently, a new approach is to perform joint optimization across the protocol stack, leading to more efficient and adaptive resource utilization. This new paradigm is called *cross-layer design*. In [1], it was shown that joint optimization of link capacity and traffic flow assignment can lead to significant performance gains in the case of supporting a single video stream over the network.

When multiple media streaming sessions are present in the network, it is also important to perform resource allocation among the different source-destination pairs. In the case of streaming compressed video content, this is characterized by the encoding rate allocated to each video stream. In this paper, we consider joint capacity, flow and rate allocation for video streaming between multiple source-destination pairs. The *capacity* assignment is a point in the capacity region that is determined by the time sharing between different transmission schemes. The *flow* assignment determines the actual data rate carried by a particular wireless link, so as to minimize overall network congestion, which reflects the amount of delay experienced by the video packets. For each source-destination pair, the allocated *rate* affects the encoded video quality of the stream, and is chosen to balance the tradeoff between video quality and incurred network congestion. Note that given the allocated rate of a stream, the video traffic is transmitted from source to destination in a multi-hop fashion, along the routes determined by the flow assignment process. This work extends our previous efforts in joint capacity and flow allocation [1] to consider multiple source-destination pairs, introducing an additional dimension (i.e., rate of each user) into the joint optimization.

The rest of the paper is organized as follows. In Section II we briefly review existing literature on cross-layer design for multimedia applications. The next section describes our wireless channel and network model as well as the video distortion model. We then formulate the joint rate, capacity and flow allocation problem in Section IV, and explain the procedures of the optimization. Section V describes our simulation results and Section VI concludes the paper.

II. Related Work

In this section we give a brief overview of recent research in the field of cross-layer design for wireless ad-hoc networks, especially for supporting multimedia applications. In [2], [3] and [4], the authors studied joint optimization of physical layer parameters like power allocation, link capacities with the higher layer parameters like routing, link scheduling and flow assignment. It was shown that the joint optimization of the parameters across traditional layers provide significant benefits over isolated optimization within a single layer. In [1] the authors describe an algorithm for joint capacity and flow allocation and demonstrate significant benefits over a competing oblivious-layer scheme, in the case of low-latency video streaming. This cross-layer model was extended across the protocol stack in [5], where a new framework for cross-layer optimization across all layers was introduced. The cross-layer approach has been exploited in joint design of distributed MAC and network coding [6] and also in sensor networks where joint optimization is done to improve the energy efficiency of sensor networks [7].

III. System Model

We consider a wireless ad-hoc network consisting of N nodes randomly deployed in a region. Each node can either be a transmitter, a receiver or a relay. The source and the destination communicate with each other in a multi-hop manner. The communication over each wireless link may suffer from interference from simultaneous neighboring transmissions. Below we describe our wireless network model which captures the effect of interference between two simultaneous transmissions. In the following subsection we describe our calculation of the capacity region based on time-sharing among basic transmission schemes. In Subsections III-C and III-D, we explain our congestion and video distortion model used for trading off encoded video quality versus network congestion in the joint optimization.

A. Wireless Network Model

The wireless channel model is characterized by three basic phenomena, namely the path loss, shadowing and fading. In this paper we focus only on the path loss model for the wireless channel. Specifically we use the two-ray ground model to characterize the channel. In this model the received power at distance d is given as [8]

$$P_r(d) = P_r(d_c)\left(\frac{d}{d_c}\right)^{-4} \tag{1}$$

where d_c is the critical distance beyond which the received power falls off proportionally with d^{-4}. From [8] we know that the critical distance is given as $d_c = 4h_r h_t/\lambda$, where h_t, h_r are the transmit and receive antenna heights and λ is the signal wavelength. The received power $P_r(d_c)$ depends on the transmit power P_t as:

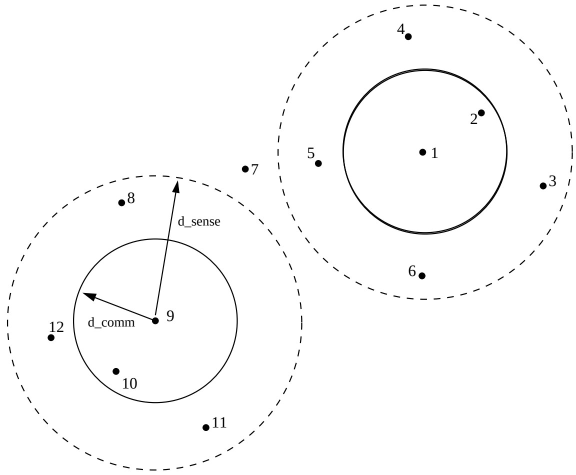

Fig. 1. Wireless network model

$$P_r(d_c) = P_t\left(\frac{\sqrt{G_l}\lambda}{4\pi d_c}\right)^2, \tag{2}$$

where $\sqrt{G_l}$ is the antenna gain.

Each node transmits with a fixed power P_t and can communicate with nodes within a region of radius d_{comm} around it. The communication radius is determined by the transmit power P_t, receiver sensitivity P_{rx} and the channel model from Eq. (1) and Eq. (2). Each node communicates with its neighbors (i.e., nodes within the distance d_{comm}) with a fixed rate R_0. To avoid interference with neighboring nodes, each node uses a carrier sense mechanism where it senses for ongoing communications before beginning its transmission. Depending upon the carrier sense sensitivity P_{cs}, each node has a region of radius d_{sense} where simultaneous communications cannot take place. Figure 1 illustrates our network model, where Node 1 can communicate with only Node 2, since it lies within distance d_{comm}. Meanwhile, all nodes within d_{sense} of Node 1 (i.e., Nodes 3, 4, 5 and 6) cannot transmit or receive when communication between Node 1 and Node 2 is ongoing. This model is similar to CSMA/CA used in 802.11 networks [9] where a node overhearing an ongoing communication refrains from its own transmission for a random backoff time.

B. Capacity Region

We define the capacity region to be the entire set of rates simultaneously achievable between pairs of nodes under a given communication protocol. This definition of capacity was first introduced in [10] and lower bounds the information theoretic capacity region (which is still an open problem). A similar definition of capacity was also used in [4] to perform resource allocation in wireless networks. Following the notation of [1] let $\mathcal{T} = \{t_1, \ldots, t_n\} \subseteq \{1, \ldots, N\}$ be the set of transmitters and $\mathcal{R} = \{r_1, \ldots, r_n\} \subseteq \{1, \ldots, N\}$ be the set of receivers which can simultaneously communicate with each other. Note that the set of transmitters $\mathcal{T}$ and the set of receivers $\mathcal{R}$ need to satisfy the feasibility conditions as described in the wireless model above. Specifically

$$d(t_i, r_i) < d_{comm} \quad \forall t_i \in \mathcal{T} \quad \forall r_i \in \mathcal{R} \tag{3}$$

which implies that the intended receiver is within d_{comm} of the transmitter. To avoid interference we also require that there are no active nodes (i.e., no nodes transmitting or receiving) within d_{sense} of the intended transmitter and receiver. That is

$$d(t_i, t_j) > d_{sense}, \quad d(r_i, t_j) > d_{sense} \quad \forall j \in \mathcal{T},\ j \neq i \tag{4}$$

$$d(t_i, r_k) > d_{sense}, \quad d(r_i, r_k) > d_{sense} \quad \forall k \in \mathcal{R},\ k \neq i \tag{5}$$

We define the tuple $\mathcal{S} = \{\mathcal{T}, \mathcal{R}\}$ satisfying the feasibility conditions (3)-(5) as the transmission scheme. For the network shown in Fig. 1, we have $\mathcal{T} = \{1, 9\}$ and $\mathcal{R} = \{2, 10\}$ and $\{\mathcal{T}, \mathcal{R}\}$ is one such basic transmission scheme. For a specific transmission scheme $\mathcal{S}_k = \{\mathcal{T}_k, \mathcal{R}_k\}$ let $\mathcal{C}_k = \{\mathcal{C}_{k,ij}\}$ be the set of achievable rates. Here

$$\mathcal{C}_{k,ij} = \begin{Bmatrix} R_0 & (i,j) \in (\mathcal{T}_k, \mathcal{R}_k) \\ 0 & otherwise \end{Bmatrix} \tag{6}$$

where R_0 is the fixed rate between any transmitter-receiver pair as given by the wireless model above. In [4], the tuple $(\mathcal{T}_k, \mathcal{R}_k, \mathcal{C}_k)$ is called the *Elementary Capacity Graph*. The capacity region $\mathcal{C}$ can thus be written as the set of rates simultaneously achievable by time sharing of different basic transmission schemes:

$$\mathcal{C} = \left\{ \sum_{k=1}^{L} \lambda_k \mathcal{C}_k : \lambda_k \geq 0, \sum_{k=1}^{L} \lambda_k \leq 1 \right\} \tag{7}$$

where L is the total number of transmission schemes given by $L = \sum_{n=1}^{\lfloor N/2 \rfloor} \frac{N!}{n!(N-2n)!}$ and λ_k are the time sharing coefficients which represent the percentage of time each of these basic transmission scheme is used.

C. Network Congestion Model

In video streaming applications, each video packet needs to arrive at the decoder by a deadline, at which time it is expected to be decoded and displayed for continuous playout of the video contents. Packets arriving after the deadline are typically treated at the decoder as if they were lost. Therefore, delivery of video packets is delay-critical, and the received video quality is affected by congestion in the network, i.e., the average queuing delay per link.

For simplicity, we use the M/M/1 queuing model to estimate congestion over each link (i, j) in the network. The total congestion in the network Δ can be evaluated as the sum of congestion at each link [11]:

$$\Delta = \sum_{(i,j)} \frac{f(i,j)}{C(i,j) - f(i,j)} \tag{8}$$

where $f(i, j)$ and $C(i, j)$ are the flow and capacity on the directed link (i, j).

Alternatively, congestion on each link is also reflected in the link utilization factor: $\rho(i, j) = f(i, j)/C(i, j)$, and congestion over the entire network is determined by the link with maximum utilization:

$$\Delta = \sum_{(i,j)} \frac{\rho(i,j)}{1 - \rho(i,j)}. \tag{9}$$

D. Video Distortion Model

In this section we present a parametric model for video distortion as a function of encoded rate of each stream. Let S be the set of video sources in a network. For each $s \in S$ we associate a mean square error (MSE) distortion D^s when the video stream (associated with the particular source) is encoded at the rate R^s. The distortion rate characteristics of each stream can be fitted to a parametric model [12].

$$D^s(R^s) = D_0^s + \frac{\theta^s}{(R^s - R_0^s)} \tag{10}$$

where D_0^s, R_0^s and θ^s depend on the actual video content and are estimated from empirical rate distortion curves using regression techniques.

Typically, the encoded video quality is evaluated in terms of *peak-signal-to-noise-ratio* (PSNR), which is related to the MSE distortion as:

$$\text{PSNR} = 10\log_{10}(255^2/\text{MSE}) \tag{11}$$

It should be noted that a good video quality implies lower value of MSE which translates to a higher value of PSNR.

IV. Joint Capacity, Flow and Rate Allocation for Multiple Users

In this section we formulate the problem of joint capacity, flow and rate allocation for multiple source-destination pairs. It is evident from the video distortion model described above that increasing the rate assigned to the flow reduces the overall distortion. However this increased rate causes congestion in the network which leads to greater proportion of late packet arrivals as well as losses due to buffer overflow. These late/lost packets typically lead to artifacts in the decoded video sequences, hence degrading end-to-end video quality. Therefore, in a bandwidth-limited network, one would expect the optimum encoding rate to lie somewhere in the middle. To find the optimal rate allocated to each source-destination pair we aim to minimize the expected Lagrangian cost given by:

$$J = \sum_{s \in S} D^s(R^s) + \alpha \Delta(\underline{R}), \tag{12}$$

where $D^s(R^s)$ is the distortion for the stream s at the rate R^s, α is the Lagrange multiplier and $\Delta(\underline{R})$ is the total network congestion in the network for the rate tuple $\underline{R} = \{R^s, s \in S\}$. By evaluating the optimal $\Delta(\underline{R})$ for all feasible rate tuples, one can, in turn, evaluate the corresponding Lagrangian costs according to Eq. (12), thus achieving joint optimization of capacity, flow and rate. We therefore first evaluate $\Delta(\underline{R})$ for all feasible rate tuples $\underline{R}$ using joint capacity and flow optimization and then find the best rate tuple which minimize the overall Lagrangian cost as given in eq. (12).

A. Joint capacity and flow optimization

We formulate the problem of joint capacity and flow allocation for *given* rate tuple $\{\underline{\tilde{R}}^s, s \in S\}$ as a convex optimization problem. From Eq. (12), it is obvious that for a given rate tuple $\underline{R}$, the first terms in the total cost is fixed, so one only needs to minimize the total congestion by finding the optimal flow and capacity allocation. Note, however, that network congestion defined in Eq. (8) is not a convex function of *both* flow and capacity. Instead, we choose to perform the capacity and flow assignment using the alternative metric of the maximum link utilization:

$$\rho\left(\mathbf{C}, \mathbf{f}\right) = \max_{(i,j)} \frac{f_{i,j}}{C_{i,j}}. \tag{13}$$

Here $f_{i,j}$ and $C_{i,j}$ are the flow and capacity on the directed link (i, j). Intuitively, this would lead to load balancing in the network, and would also prevent any bottleneck links from congesting the network. As pointed out in [13], minimizing maximum link utilization leads to solutions of properties similar to that from congestion minimization. This was also the optimization objective used in [1] to perform the capacity and flow allocation for the single user case. This performance measure $\rho\left(\mathbf{C}, \mathbf{f}\right)$ is also a quasi-convex function of *both* flow $\mathbf{f}$ and capacity $\mathbf{C}$ [1]. The following set of equalities show that the sub-level sets of the function are convex [1]:

$$\begin{aligned} & \left\{(\mathbf{C}, \mathbf{f}) \;\middle|\; \rho\left(\mathbf{C}, \mathbf{f}\right) \leq \gamma\right\} & (14)\\ = & \left\{(\mathbf{C}, \mathbf{f}) \;\middle|\; \max_{(\mathbf{i},\mathbf{j})} \frac{\mathbf{f_{i,j}}}{\mathbf{C_{i,j}}} \leq \gamma\right\} & (15)\\ = & \left\{(\mathbf{C}, \mathbf{f}) \;\middle|\; \mathbf{f_{i,j}} - \gamma \mathbf{C_{i,j}} \leq \mathbf{0}, \forall (\mathbf{i}, \mathbf{j})\right\}. & (16) \end{aligned}$$

This implies that the optimal solution can be obtained by finding the smallest γ for which a solution exists. This can be done using the bisection method as described in [14]. The feasibility conditions on $f_{i,j}$ and $C_{i,j}$ can be expressed as a set of linear constraints.

Let S be the set of all sources in the network, and D the set of corresponding destination nodes. We denote the flow over link (i, j) due to stream with source node s as f^s_{ij}. Note that the total flow on each link includes contributions from all streams: $f_{ij} = \sum_s f^s_{ij}$. For the given rate tuple $\underline{\tilde{R}} = \{\tilde{R}^s, s \in S\}$, the following set of constraints represent the flow conservation equations over each node, for each stream s:

$$\begin{aligned} \sum_j f^s_{sj} - \sum_j f^s_{js} &= \tilde{R}^s \quad \forall s \in S & (17)\\ \sum_j f^s_{dj} - \sum_j f^s_{jd} &= -\tilde{R}^s \quad \forall d \in D & (18)\\ \sum_j f^s_{kj} - \sum_j f^s_{jk} &= 0 \quad \forall k \notin (S \cup D) & (19) \end{aligned}$$

Equation (17) tells that the difference between the total outgoing flow and total incoming flow at a source node should be equal to the total rate of the encoder. Similar flow conservation equation holds for the destination node and for all relay nodes, where the total incoming flow should be equal to the total outgoing flow (18)-(19). Since the flow and capacity values at each link (i, j) are positive numbers we have:

$$\begin{aligned} f^s_{ij} &\geq 0 \quad \forall (i,j) \quad \forall s \in S & (20)\\ C_{ij} &\geq 0 \quad \forall (i,j). & (21) \end{aligned}$$

We also require that the capacity matrix $\mathbf{C}$ should lie inside the capacity region given by Eq. (7). This can be expressed as the set of linear constraints:

$$\mathbf{C} = \mathcal{C}\mathbf{\Lambda}, \tag{22}$$

where Λ is the set of time sharing coefficients λ_k and $\mathcal{C}$ is the set of basic transmission schemes expressed by Eq. (6). The constraints on these time sharing coefficients are:

$$\begin{aligned} \lambda_k &\geq 0 & (23)\\ \sum_k \lambda_k &\leq 1. & (24) \end{aligned}$$

The optimization function is thus to find the minimum γ such that $f_{i,j} - \gamma C_{i,j} \leq 0, \forall (i, j)$ and the constraints (17) - (24) are satisfied. Note that this optimization function gives the optimal flow and capacity assignment for each link (i, j) for a given set of rate tuples $\underline{\tilde{R}}^s$.

B. Oblivious-layer capacity and flow assignment

As a competing scheme, we also present an algorithm for allocation of capacity and flow with oblivious layers. In this architecture, the bidirectional links between nodes that are within the distance d_{comm} of each other are established. The network topology shown in Fig. 2 shows these bidirectional links.

The capacity assignment assigns equal share to all basic transmission schemes. Thus the time sharing coefficients λ_k as given in Eq. (7) are all equal. This capacity assignment is

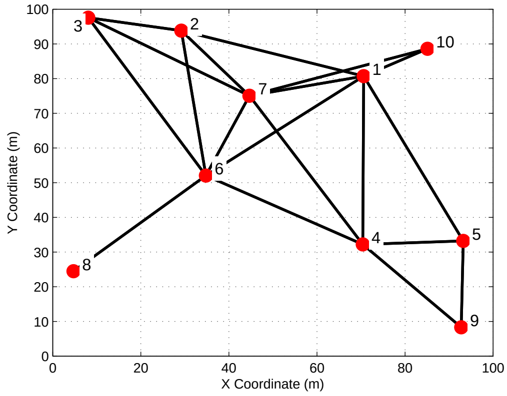

Fig. 2. Network topology

[1]A function is quasi-convex if the domain over which its value is below a threshold (called sub-level set) is convex [14].

completely oblivious of the encoding rate at each source as well as the total traffic carried by each link. The optimal flow assignment is then done for the given capacity allocation. The constraints on the flow assignment include the flow conservation equations (17)-(19) and flow positivity constraints given by Eq. (20).

In next section, we present our simulation results for joint capacity, flow and rate allocation using the model and equations developed in this section. Specifically, we use Eq. (16) - Eq. (24) to perform the joint capacity and flow allocation. The flows and capacities at each link are then used to determine the total congestion as given in Eq. (9). This congestion value is then used in Eq. (13) to determine the Lagrangian cost.

V. Simulation Results

A. Simulation scenario

We consider an ad-hoc network consisting of 10 nodes within an 100m-by-100m square. Numerical simulations are performed in Matlab. The network topology used for the simulation results is shown in Figure. 2. Each node transmits with the power P_t = 15 dBm (0.316 mW), with receiver sensitivity P_{rx} = -87 dBm (2.0×10^{-9} mW) and carrier sense sensitivity P_{cs} = -100 dBm (1.0×10^{-10} mW). The antenna gain is $G_l = 0.05$ and the critical distance is calculated as $d_c = 10.07$ m, for antenna height of 1.0 m. According to Eq. (1) and (2), the communication radius d_{comm} is 53 m and the sensing radius d_{sense} is 112.22 m. Each node communicates with its neighbors with a fixed rate $R_0 = 2.5$ Mbps [2]. Note that the values of d_{comm} and d_{sense} imply that the chosen network topology allows no spatial reuse. This is because the sensing distance is large and it prevents any simultaneous communication in the network.

Two video streams are sent over different source-destination pairs. The first video stream is set up from Node 3 to Node 5 and consists of the *Foreman* video sequence, containing relatively high motion in the content. Given the network topology and transmission ranges, note that multi-hop transmissions are needed for each streaming session. In our simulation, it is observed that each streams travels over 3 hops, along a route extracted from the flow assignment results [3].

The second video stream from Node 8 to Node 9 is the *Mother and Daughter* sequence, with slow motion and static background. Both sequences are of the CIF format, with picture size 352×288 pixels per frame and playing at 30 frames per second. The rate-distortion curves in Fig. 3 are derived from empirical encodings using the H.264/AVC reference codec [15]. As is evident from the figure, the two video streams have different characteristics and hence would need different encoding rates to achieve the same distortion. Specifically, for the same decoding quality, the *Foreman* sequence requires a much higher rate as compared to the *Mother and Daughter* sequence, since more efficient compression can be achieved for the latter.

[2]This corresponds to the effective bandwidth of transmitting packets of 1000 bytes over an 802.11b network with data rate 2.5 Mbps.

[3]Interested readers are referred to [1] for a detailed account of the route extraction process.

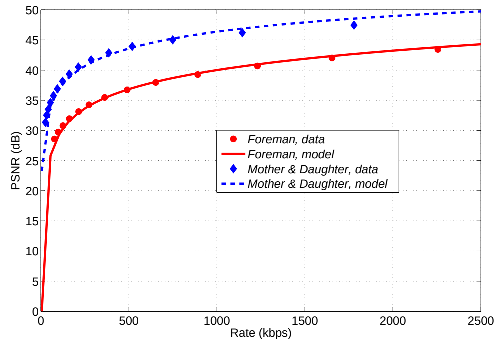

Fig. 3. PSNR-rate curves of *Foreman* and *Mother and Daughter* video sequences. Experimental data points are fitted to the video distortion model given in Section III-D

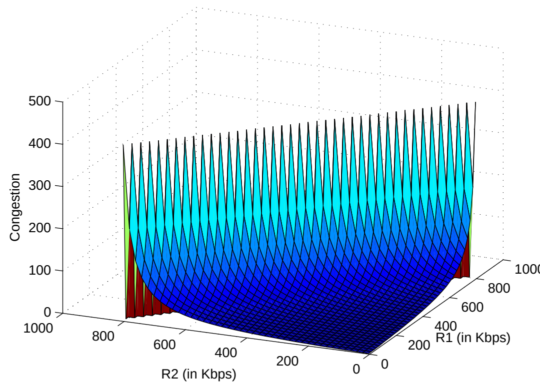

Fig. 4. Total network congestion vs. encoding rates of two users

B. Joint optimization

We first present results for the case of joint capacity and flow allocation. Figure 4 presents the surface plot of the overall network congestion as a function of target rates R^1 and R^2 when both the capacities and flows are jointly optimized. As the encoding rates of the two streams are increased, the network becomes more and more congested. Also the overall link utilization is increased and approaches unity at the boundary of the feasible region of the rate pairs. It can be seen that the maximum individual rate that each stream can support is about 830 Kbps. However the presence of the second stream lowers the actual sustainable rate of the first stream.

Figure 5 presents the contour plot of the total Lagrangian cost for a specific value of Lagrange multiplier $\alpha = 0.5$. As can be observed, the optimal encoding rates for two streams lie within the rate region. Figure 6 plots the optimal encoding rates for two streams for different values of Lagrange multiplier from $\alpha = 1$ to $\alpha = 10$. As can be observed from

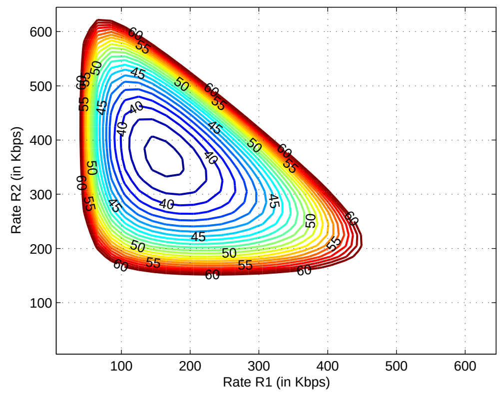

Fig. 5. Combined cost vs. encoding rates of two users for Lagrange multiplier $\alpha = 0.5$

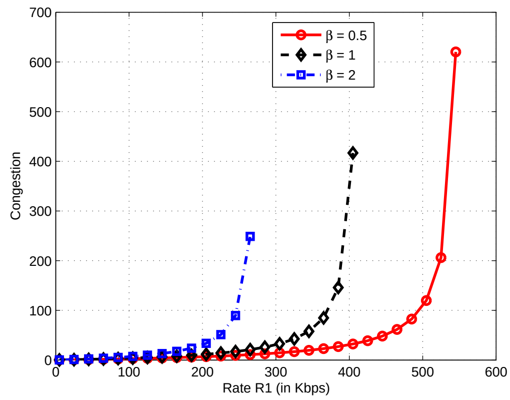

Fig. 7. Total network congestion as a function of encoding rate R^1. The rate of the second stream $R^2 = \beta R^1$

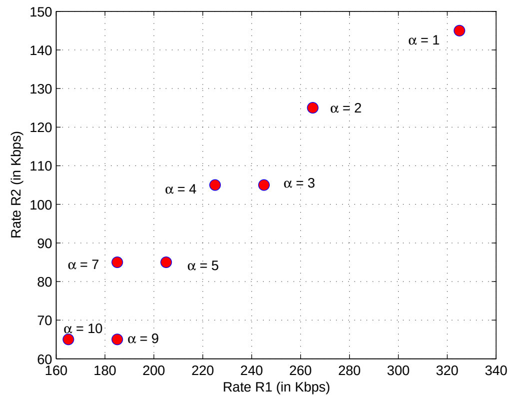

Fig. 6. Optimal encoding rates for two streams for different values of Lagrange multiplier

TABLE I

OPTIMAL ENCODING RATE R^1 IN (KBPS)

	α = 1	α = 2	α = 10
β = 0.5	305	205	165
β = 1	245	165	125
β = 2	165	125	105

the graph, the optimal encoding rates decrease with increasing α. This is because, as the Lagrange multiplier is increased, the combined cost is more affected by increasing congestion and hence the optimal encoding rates are reduced.

In order to better present the result, and to draw meaningful conclusions, we restrict out attention to certain 2-dimensional slices of this 3-dimensional plot. In particular we restrict our attention to cases where the encoding rates of the second stream R^2 are proportional to the encoding rate of the first stream R^1, i.e., we have $R^2 = \beta R^1$, where $\beta \in \{0.5, 1, 2\}$. Figure 7 plots the total network congestion as a function of encoding rate R^1. Thus the maximum rate sustained for the first stream R^1 is lowered as the encoding rate of the second stream R^2 is increased. Intuitively this is reasonable since the lack of spatial reuse forces the two streams to time-share the overall capacity. This also means that the capacity region is just the linear combination of the maximum sustainable rate of either of the two streams and hence is triangular in shape.

We now plot the total Lagrangian cost in Eq. (12) for different values of the weighting factor $\alpha \in \{1, 5, 10\}$. For clarity we again restrict our focus to cases where R^2 is proportional to R^1. Figures 8 presents the total cost as a function of R^1 for β = 0.5, 1 and 2 respectively. Initially, the total cost decreases as the encoding rate is increased. This is primarily due to decreased distortion as given by Eq. (10). However when the rates are increased beyond a certain point, the overall congestion causes the total cost to increase. Thus there exists an optimal encoding rate.

Table I gives the optimal encoding rate R^1 for different values of α and β. It is evident from the table that as the weighting factor α is increased, the optimal rate becomes less, leading to a more conservative allocation of rate. When β is larger the optimal encoding rate for stream 1 is decreased. This is because the larger value of β implies that the corresponding encoding rate R^2 is large, thereby increasing the total traffic rate and congestion in the network.

C. Comparison with oblivious-layer allocation

In this subsection we compare the joint optimization algorithm with oblivious-layer allocation. Figure 9 shows the network congestion as a function of encoding rate for both the joint optimization as well as the oblivious layer case. Given the same target rate pairs, it is evident from the figure that the overall congestion is much lower when the capacities and flows are jointly optimized. As a consequence, the maximum sustainable rate is significantly decreased for the oblivious layer scheme. For example, when the encoding rates R^1 and R^2 are equal (i.e., β = 1), the maximum sustainable encoding rate with joint optimization is about 400 Kbps (see Fig. 7). This maximum sustainable rate is decreased to about 60 Kbps for oblivious layer allocation.

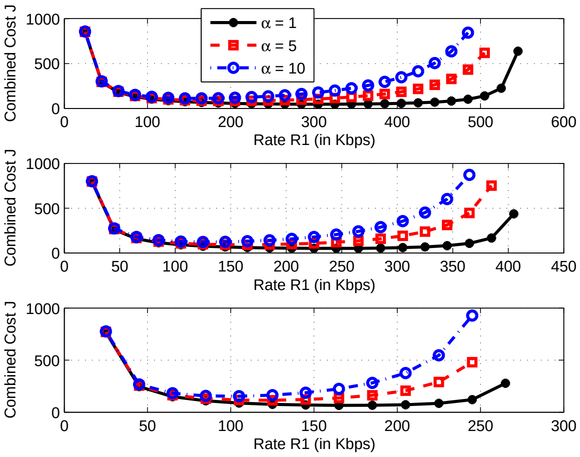

Fig. 8. Combined Lagrangian Cost as a function of encoding rate R^1. The rate of the second stream is $R^2 = \beta R^1$, where $\beta \in \{0.5, 1, 2\}$

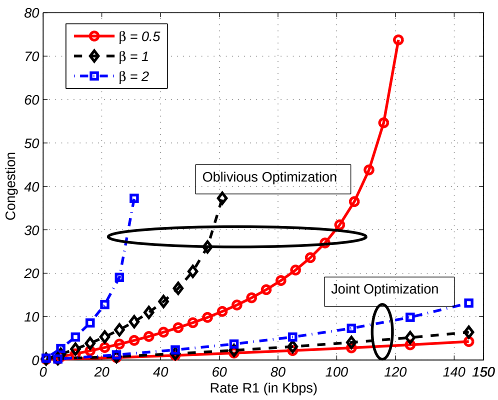

Fig. 9. Comparison of network congestion for oblivious layer optimization as well as joint optimization

As an another comparison, Table II gives the supportable video quality for both joint optimization as well as oblivious layer optimization. The overall supportable video quality is reduced by about 5 dB for the oblivious layer case, due to the much lower sustainable rate as compared to the joint optimization.

VI. Conclusions

We presented an algorithm for joint capacity, flow and rate allocation for supporting video streaming over wireless networks. In particular we considered multiple video streams in the network and performed joint allocation over the application layer (encoding rate of video), network layer (flow assignment to each link) and MAC layer (capacity allocation to each link). The objective is to minimize the total Lagrangian cost of total video distortion and overall network congestion. Our simulation results shown a significant performance gain over a scheme with oblivious-layer allocation, improving the maximum sustainable video rate by 4-6 times, and encoded quality by up 5 dB in PSNR.

TABLE II

Table of supportable video quality and associated rate. The encoding rate of the second stream is $R^2 = 0.5R^1$

		α = 1	α = 5	α = 10
Joint	PSNR (in dB)	33.11	31.29	30.28
	Rate (in Kbps)	305	205	165
Oblivious	PSNR (in dB)	28.15	26.80	25.72
	Rate (in Kbps)	106	81	66

Acknowledgment

The authors would like to thank Taesang Yoo and Eric Setton at Stanford University for many insightful discussions.

References

[1] T. Yoo, E. Setton, X. Zhu, A. Goldsmith, and B. Girod, "Cross-layer design for video streaming over wireless ad-hoc networks," in *Proc. of International Workshop on Multimedia Signal Processing (MMSP)*, Siena, Italy, September 2004, pp. 99–102.

[2] R. Cruz and A. Santhanam, "Optimal routing, link scheduling and power control in multi-hop wireless networks," in *Proc. of INFOCOM*, San Francisco, USA, March 2003, pp. 702–711.

[3] L. Xiao, M.Johansson, and S. Boyd, "Simultaneous routing and resource allocation via dual decomposition," *IEEE Transactions on Communications*, vol. 52, no. 7, pp. 1136–1144, July 2004.

[4] Y. Wu, P. A. Chou, Q. Zhang, K. Jain, W. Zhu, and S.-Y. Kung, "Network planning in wireless ad-hoc networks : A cross-layer approach," *IEEE Journal on Selected Areas in Communications*, vol. 23, no. 1, pp. 136–150, January 2005.

[5] E. Setton, T. Yoo, X. Zhu, A. Goldsmith, and B. Girod, "Cross-layer design of ad hoc networks for real-time video streaming," *IEEE Wireless Communications Magazine*, vol. 12, no. 4, pp. 59–65, August 2005.

[6] Y. E. Sagduyu and A. Ephremides, "Crosslayer design for distributed MAC and network coding in wireless ad hoc networks," in *Proc. of International Symposium on Information Theory (ISIT)*, Adelaide, Australia, September 2005, pp. 1863–1867.

[7] S. Cui, R. Madan, A. Goldsmith, and S. Lall, "Joint routing, MAC, and link-layer optimization in sensor networks with energy constraints," in *Proc. of International Conference on Communications (ICC)*, Seoul, Korea, May 2005, pp. 725–729.

[8] A. Goldsmith, *Wireless Communications*. Cambridge University Press, 2005.

[9] *IEEE Standard for Wireless LAN Medium Access Control (MAC) and Physical Layer (PHY) Specifications, P802.11*, Nov. 1997.

[10] S. Toumpis and A. Goldsmith, "Capacity regions for wireless ad hoc networks," *IEEE Transactions on Wireless Communications*, vol. 2, no. 4, pp. 736–748, July 2003.

[11] L. Kleinrock, *Queuing Systems, Volume II: Computer Applications*. N.Y.: Wiley-Interscience, 1976.

[12] K. Stuhlmuller, N. Farber, M. Link, and B. Girod, "Analysis of video transmission over lossy channels," *IEEE Journal on Selected Areas in Communications*, vol. 18, no. 6, pp. 1012–1032, June 2000.

[13] D. Berteskas and R. Gallager, *Data Networks*. NJ: Prentice Hall, 1987.

[14] S. P. Boyd and L. Vandenberghe, *Convex Optimization*. Cambridge University Press, 2005.

[15] *Advanced Video Coding for Generic Audiovisual services, ITU-T Recommendation H.264 - ISO/IEC 14496-10(AVC)*, ITU-T and ISO/IEC JTC 1, 2003.